



Supplement of

Humidity changes and possible forcing mechanisms over the last millennium in arid Central Asia

Shengnan Feng et al.

Correspondence to: Xingqi Liu (xqliu@cnu.edu.cn)

The copyright of individual parts of the supplement might differ from the article licence.

Supplement of materials and methods

Microscope observation analysis

Four random samples for microscope observation were pretreated with 30 mL of 20% H₂O₂ to remove organic matter and then with 30 mL of 20% HCl to remove carbonates, then the samples rinsed with deionized water to neutral and dried at below 40 °C in a constant temperature air-blast drying oven. Finally, samples sifted by 30-mesh and 115-mesh sieve were used for microscope observation.

Model settings

We used the transient experiment for the last millennium with only the TSI forcing using the Max Planck Institute Earth System Model (MPI-ESM) (Jungclaus et al., 2014). The simulation grid of 42.67°N, 82.50°E was selected because it is the nearest site to Lake Dalongchi. The output variables of the MPI-ESM include the surface air temperature, precipitation, evaporation, and effective humidity. Given that most of the precipitation in the study area occurs in summer (Lan et al., 2018) and the evaporation processes are intensified in summer seasons, we mainly considered the simulated results of June-July-August (JJA).

Supplementary Figures

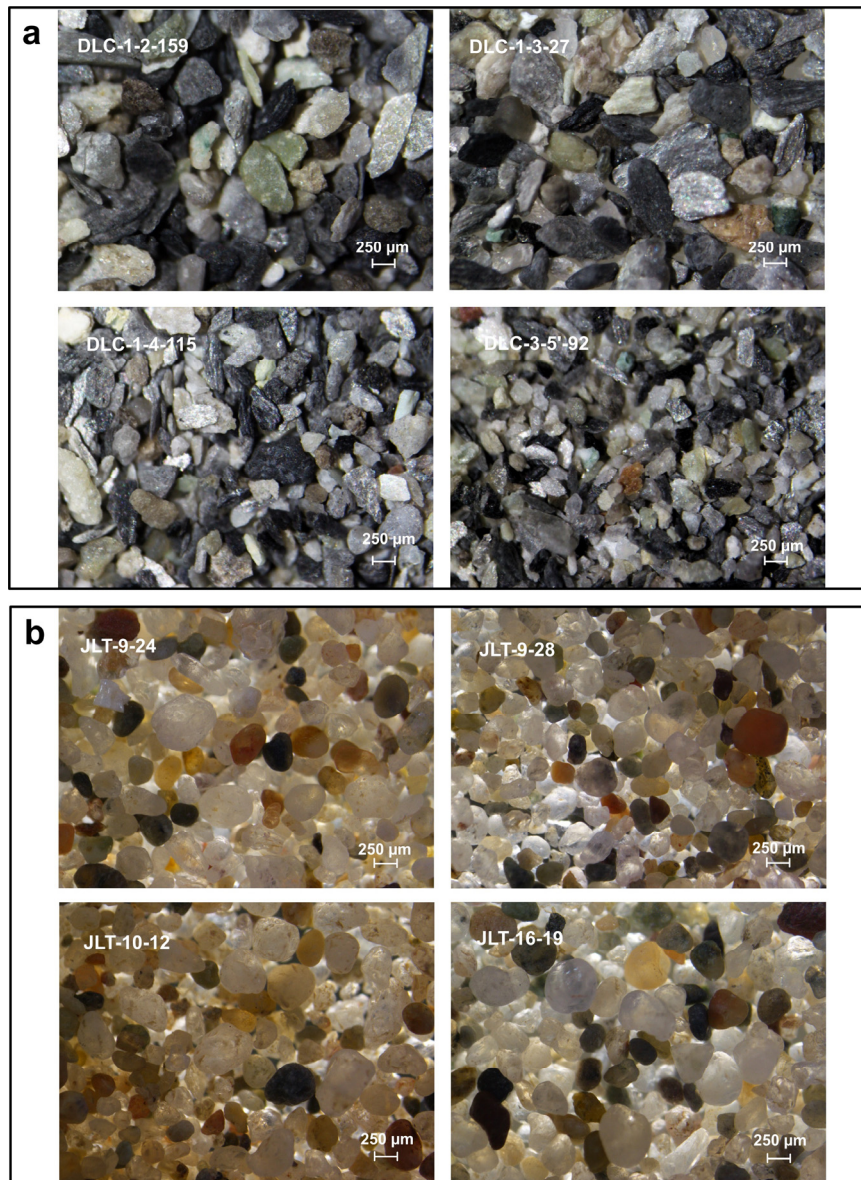


Figure S1. The photomicrograph comparison of 125-500 μm size-fractions in Lake Dalongchi and the typical eolian sand in Jilantai Salt Lake. (a) The 125-500 μm size-fractions from randomly selected samples of DLC1819 core. (b) The typical eolian sand from randomly selected samples of JLT-2010 core (Zhang et al., 2021).

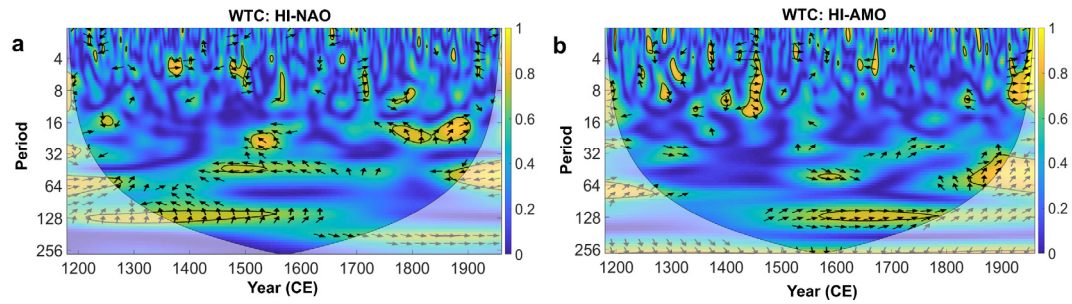


Figure S2. Wavelet coherence (WTC) analysis between the HI and the NAO and AMO. (a) The WTC result between the HI and NAO (Ortega et al., 2015). (b) The WTC result between the HI and AMO (Wang et al., 2017). The 95% confidence level against red noise is shown as an irregular thick black contour and the thin curved black solid line is the cone of influence (COI). The outside results might be affected by the edge effects of zero paddings. The black arrows illustrate the relative phase relationship: arrows pointing right are in-phase and those pointing left are anti-phase. The 95% significant confidence level of the WTC is calculated using Monte Carlo methods (Grinsted et al., 2004).

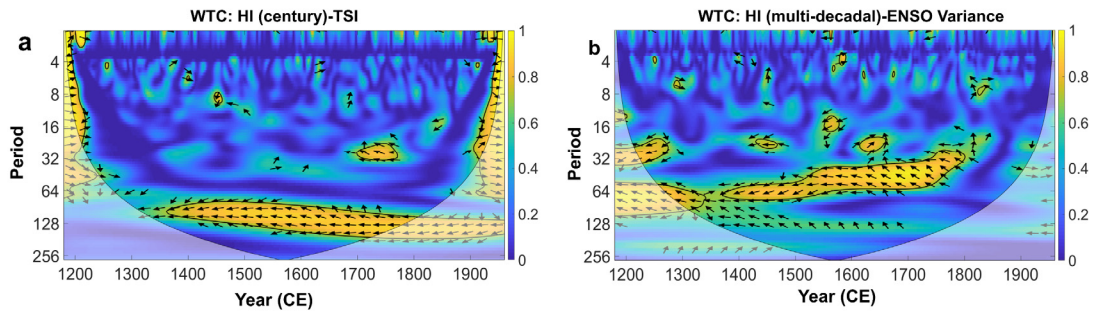


Figure S3. The WTC analysis between the extracted HI components and the TSI and ENSO. (a) The WTC between the century component of the HI and TSI reconstruction (Bard et al., 2000). (b) The WTC between the multidecadal component of the HI and ENSO 21-yr variance (Li et al., 2011). The 95% confidence level against red noise is shown as an irregular thick black contour and the thin curved black solid line is the cone of influence (COI). The outside results might be affected by the edge effects of zero paddings. The black arrows illustrate the relative phase relationship: arrows pointing right are in-phase and those pointing left are anti-phase. The 95% significant confidence level of the WTC is calculated using Monte Carlo methods (Grinsted et al., 2004).

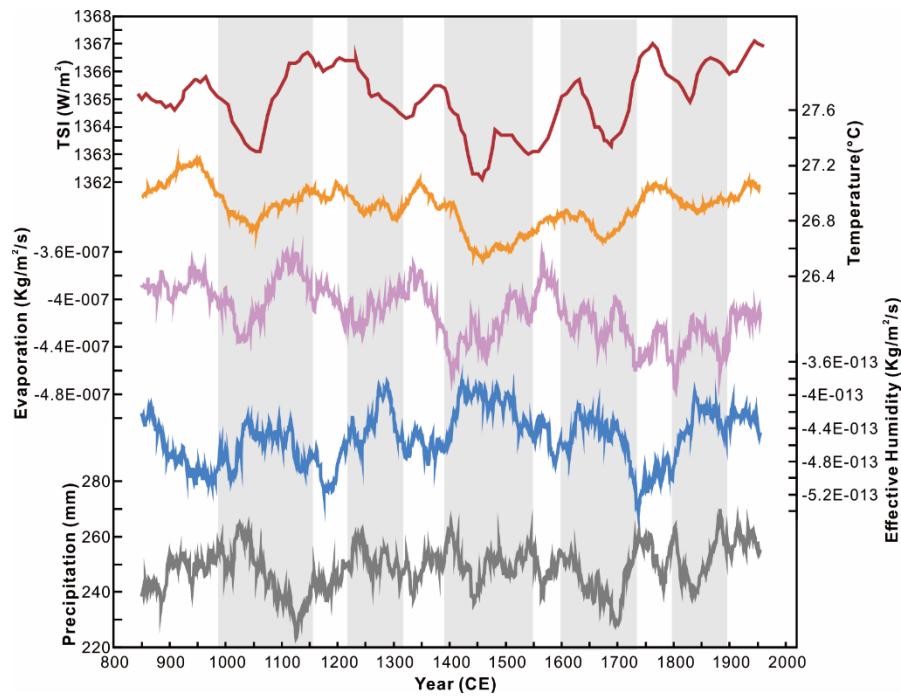


Figure S4. The results of the transient experiment forced only by the TSI. All the annual resolution series are presented by a 101-year running average to isolate century-scale variability. The light grey bars indicate the high-value period of relative humidity.

Reference

- Bard, E., Raisbeck, G., Yiou, F., and Jouzel, J.: Solar irradiance during the last 1200 years based on cosmogenic nuclides, *Tellus B: Chemical and Physical Meteorology*, 52, 985-992, 10.1034/j.1600-0889.2000.d01-7.x, 2000.
- Grinsted, A., Moore, J. C., and Jevjeva, S.: Application of the cross wavelet transform and wavelet coherence to geophysical time series, *Nonlinear Processes in Geophysics*, 11, 561-566, 10.5194/npg-11-561-2004, 2004.
- Jungclaus, J. H., Lohmann, K., and Zanchettin, D.: Enhanced 20th-century heat transfer to the Arctic simulated in the context of climate variations over the last millennium, *Climate of the Past*, 10, 2201-2213, 10.5194/cp-10-2201-2014, 2014.
- Lan, J., Xu, H., Sheng, E., Yu, K., Wu, H., Zhou, K., Yan, D., Ye, Y., and Wang, T.: Climate changes reconstructed from a glacial lake in High Central Asia over the past two millennia, *Quaternary International*, 487, 43-53, 10.1016/j.quaint.2017.10.035, 2018.
- Li, J., Xie, S.-P., Cook, E. R., Huang, G., D'Arrigo, R., Liu, F., Ma, J., and Zheng, X.-T.: Interdecadal

- modulation of El Niño amplitude during the past millennium, *Nature Climate Change*, 1, 114-118, 10.1038/NCLIMATE1086, 2011.
- Ortega, P., Lehner, F., Swingedouw, D., Masson-Delmotte, V., Raible, C. C., Casado, M., and Yiou, P.: A model-tested North Atlantic Oscillation reconstruction for the past millennium, *Nature*, 523, 71-74, 10.1038/nature14518, 2015.
- Wang, J., Yang, B., Ljungqvist, F. C., Luterbacher, J., Osborn, Timothy J., Briffa, K. R., and Zorita, E.: Internal and external forcing of multidecadal Atlantic climate variability over the past 1,200 years, *Nature Geoscience*, 10, 512-517, 10.1038/NGEO2962, 2017.
- Zhang, M., Liu, X., Yu, Z., and Wang, Y.: Paleolake evolution in response to climate change since middle MIS 3 inferred from Jilantai Salt Lake in the marginal regions of the ASM domain, *Quaternary International*, 10.1016/j.quaint.2021.06.017, 2021.